Physics Letters B 720 (2013) 181–187

Contents lists available at SciVerse ScienceDirect

Physics Letters B

www.elsevier.com/locate/physletb

The new F_L measurement from HERA and the dipole model

Carlo Ewerz [a,b,*], Andreas von Manteuffel [c,d], Otto Nachtmann [a], André Schöning [e]

[a] Institut für Theoretische Physik, Universität Heidelberg, Philosophenweg 16, D-69120 Heidelberg, Germany
[b] ExtreMe Matter Institute EMMI, GSI Helmholtzzentrum für Schwerionenforschung, Planckstraße 1, D-64291 Darmstadt, Germany
[c] Institut für Theoretische Physik, Universität Zürich, Winterthurerstr. 190, CH-8057 Zürich, Switzerland
[d] Institut für Physik (THEP), Johannes-Gutenberg-Universität, D-55099 Mainz, Germany
[e] Physikalisches Institut, Universität Heidelberg, Im Neuenheimer Feld 226, D-69120 Heidelberg, Germany

ARTICLE INFO

Article history:
Received 10 March 2012
Received in revised form 24 January 2013
Accepted 7 February 2013
Available online 8 February 2013
Editor: J.-P. Blaizot

ABSTRACT

From the new measurement of F_L at HERA we derive fixed-Q^2 averages $\langle F_L/F_2\rangle$. We compare these with bounds which are rigorous in the framework of the standard dipole picture. The bounds are sharpened by including information on the charm structure function $F_2^{(c)}$. Within the experimental errors the bounds are respected by the data. But for 3.5 GeV$^2 \leqslant Q^2 \leqslant 20$ GeV^2 the central values of the data are close to and in some cases even above the bounds. Data on F_L/F_2 significantly exceeding the bounds would rule out the standard dipole picture at these kinematic points. We discuss, furthermore, how data respecting the bounds but coming close to them can give information on questions like colour transparency, saturation and the dependencies of the dipole-proton cross section on the energy and the dipole size.

1. Introduction

Recently new results for the structure functions F_L and F_2 of deep inelastic electron– and positron–proton scattering (DIS) have been published by the H1 Collaboration [1]. In this Letter we compare these results with predictions of the popular colour-dipole model of DIS. That is, we investigate if the data respect certain bounds for the ratios of structure functions. These bounds are rigorous predictions of the standard dipole model and rely only on the non-negativity of the dipole-proton cross section.

The kinematics of $e^{\pm}p$ scattering is well known, see for instance [1,2]. The reaction is

$$e^{\pm}(k) + p(p) \to e^{\pm}(k') + X(p') \tag{1}$$

and we use the variables

$$q = k - k' = p' - p, \qquad Q^2 = -q^2,$$
$$W^2 = (p+q)^2, \qquad x = \frac{Q^2}{2pq} = \frac{Q^2}{W^2 + Q^2 - m_p^2}. \tag{2}$$

The measured structure functions F_2 and F_L are related to the cross sections σ_T and σ_L for absorption of transversely or longitudinally polarised virtual photons by

$$F_2(x, Q^2) = \frac{Q^2}{4\pi^2\alpha_{\rm em}}(1-x)\big[\sigma_T(x, Q^2) + \sigma_L(x, Q^2)\big],$$
$$F_L(x, Q^2) = \frac{Q^2}{4\pi^2\alpha_{\rm em}}(1-x)\sigma_L(x, Q^2). \tag{3}$$

Here Hand's convention [3] for the virtual-photon flux factor is used and terms of order m_p^2/W^2 are neglected. For low to moderate values of Q^2 the dipole picture for DIS [4–6] is frequently used to describe the data. For various applications of the dipole model see for instance [7–27]. In [28,29] this dipole picture was thoroughly examined using functional methods of quantum field theory. In particular, the assumptions were spelled out which one has to make in order to arrive at the standard-dipole-model formulae[1] for σ_T and σ_L or, equivalently, F_2 and F_L,

$$F_2(x, Q^2) = \frac{Q^2}{4\pi^2\alpha_{\rm em}}(1-x)\sum_q \int {\rm d}^2 r \big[w_T^{(q)}(r, Q^2) + w_L^{(q)}(r, Q^2)\big]\hat{\sigma}^{(q)}(r, \xi),$$

* Corresponding author at: Institut für Theoretische Physik, Universität Heidelberg, Philosophenweg 16, D-69120 Heidelberg, Germany.
E-mail addresses: C.Ewerz@thphys.uni-heidelberg.de (C. Ewerz), manteuffel@uni-mainz.de (A. von Manteuffel), O.Nachtmann@thphys.uni-heidelberg.de (O. Nachtmann), schoening@physi.uni-heidelberg.de (A. Schöning).

0370-2693
http://dx.doi.org/10.1016/j.physletb.2013.02.013

[1] One of these assumptions is that the dipole-proton cross section is independent of the longitudinal momentum fraction of the quark in the dipole. Lifting this assumption, as is done for example in [21,22,26], would lead to a modification of the bounds that we discuss here.

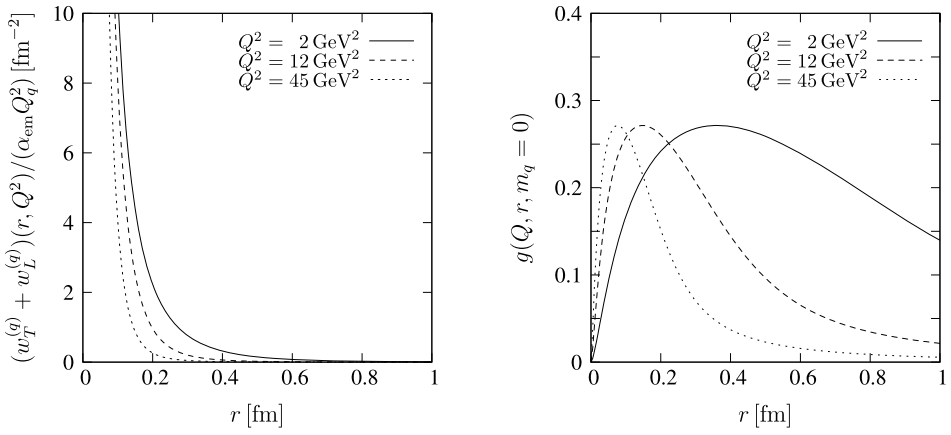

Fig. 1. The functions $\frac{1}{\alpha_{\mathrm{em}} Q_q^2}(w_T^{(q)} + w_L^{(q)})(r, Q^2)$ (left) and $g(Q, r, m_q)$ (right) versus r, both for three fixed values of Q^2 and for quark mass $m_q = 0$; see (4) and (9).

$$F_L(x, Q^2) = \frac{Q^2}{4\pi^2 \alpha_{\mathrm{em}}}(1-x) \sum_q \int \mathrm{d}^2 r\, w_L^{(q)}(r, Q^2)\, \hat{\sigma}^{(q)}(r, \xi), \tag{4}$$

see Section 6 of [29]. The charm structure function $F_2^{(c)}$ is given by the charm quark contribution to F_2. In (4) $w_{T,L}^{(q)}$ are the probability densities for the virtual photon γ^* splitting into a quark–antiquark pair of flavour q and transverse separation r. Their standard expressions are given in Appendix A. An integration over the quark's longitudinal momentum is performed. The cross section for the $q\bar{q}$ pair scattering on the proton is denoted by $\hat{\sigma}^{(q)}(r, \xi)$. This cross section depends on r and an energy variable ξ the choice of which is left open here. In [28–32] it was argued that the correct variable to choose is $\xi = W$. However, in the literature the energy variable used most frequently in the dipole cross section is $\xi = x$.

In the standard-dipole-model formulae (4) the densities $w_{T,L}^{(q)}$ are known (see Appendix A) but the dipole-proton cross sections $\hat{\sigma}^{(q)}$ have to be taken from a model. In the following we shall only use that they have to be non-negative,

$$\hat{\sigma}^{(q)}(r, \xi) \geqslant 0. \tag{5}$$

We emphasise that throughout this Letter we use the terms "standard dipole model" or, for brevity, "dipole model", to represent all models satisfying (4), (5) and (29) to (32) of Appendix A. It is this class of models we want to consider. The structure of the above equations allows to derive a non-trivial upper bound, valid in any dipole model, on the ratio

$$R(x, Q^2) = \frac{\sigma_L(x, Q^2)}{\sigma_T(x, Q^2)}; \tag{6}$$

see [29,30]. Equivalently, one can obtain a non-trivial upper bound on the ratio

$$\frac{F_L(x, Q^2)}{F_2(x, Q^2)} = \frac{R(x, Q^2)}{1 + R(x, Q^2)}. \tag{7}$$

This bound can be substantially improved if information on the charm structure function $F_2^{(c)}(x, Q^2)$ is included [31]. There is then an allowed domain, again valid in any dipole model, for the two-dimensional vector

$$\vec{V}(x, Q^2) = \begin{pmatrix} F_L(x, Q^2)/F_2(x, Q^2) \\ F_2^{(c)}(x, Q^2)/F_2(x, Q^2) \end{pmatrix}. \tag{8}$$

It is the purpose of this Letter to confront the dipole-model bounds on F_L/F_2 and on the vector $\vec{V}(x, Q^2)$ with the new HERA results [1]. This is done in Section 2. In Section 3 we discuss the results, and we give a summary in Section 4.

2. The standard-dipole-model bounds and the data

We discuss first the bound for the ratio F_L/F_2 of (7). For this we define

$$g(Q, r, m_q) = \frac{w_L^{(q)}(r, Q^2)}{w_T^{(q)}(r, Q^2) + w_L^{(q)}(r, Q^2)}, \tag{9}$$

where m_q is the mass of the quark q. For the case of massless quarks, $m_q = 0$, Fig. 1 shows $\frac{1}{\alpha_{\mathrm{em}} Q_q^2}(w_T^{(q)} + w_L^{(q)})(r, Q^2)$ and $g(Q, r, 0)$ as functions of r for three different values of $Q = \sqrt{Q^2}$ (compare Fig. 10 of [29] for a similar plot of the function $(w_L^{(q)}/w_T^{(q)})(r, Q^2)$). Note that $(w_T^{(q)} + w_L^{(q)})(r, Q^2)$ is monotonously decreasing with r. Its behaviour for small and large r is as follows for $m_q = 0$:

$$\begin{aligned} (w_T^{(q)} + w_L^{(q)})(r, Q^2) &\propto \frac{1}{r^2} \quad \text{for } r \to 0, \\ (w_T^{(q)} + w_L^{(q)})(r, Q^2) &\propto \frac{1}{r^4} \quad \text{for } r \to \infty. \end{aligned} \tag{10}$$

For a derivation of these results and for the case $m_q \neq 0$ see Appendix A of [32]. For massless quarks the function g depends only on the dimensionless variable

$$z = Q r, \tag{11}$$

such that we can write

$$\tilde{g}(z) = g(Q, r, 0). \tag{12}$$

The function $\tilde{g}(z)$ has a maximum at

$$z_m = 2.5915 \tag{13}$$

with

$$\tilde{g}(z_m) = 0.27139. \tag{14}$$

It was shown in [31] that

$$g(Q, r, m_q) \leqslant \tilde{g}(z_m) \tag{15}$$

for all $Q \geqslant 0$, $r \geqslant 0$ and $m_q \geqslant 0$. Using then (5) the dipole-model formulae (4) lead to the bound

$$\frac{F_L(x, Q^2)}{F_2(x, Q^2)} \leqslant \tilde{g}(z_m) = 0.27139. \tag{16}$$

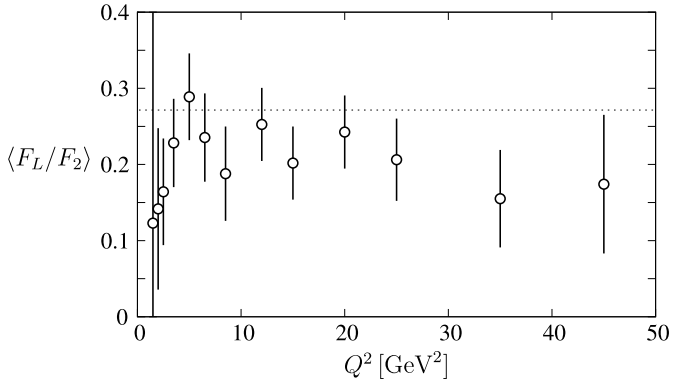

Fig. 2. The data for the fixed-Q^2 averages $\langle F_L/F_2 \rangle$ confronted with the dipole-model upper bound (16) represented by the dotted line. The data are extracted from [1].

We note that the bound (16) for F_L/F_2 is equivalent to the bound for R (6) derived in [30,31],

$$R(x, Q^2) \leqslant \frac{\tilde{g}(z_m)}{1 - \tilde{g}(z_m)} = 0.37248. \tag{17}$$

Data for F_L and F_2 at the same kinematic points are presented in [1] for Q^2 values ranging from 1.5 to 45 GeV^2. The data for the same Q^2 value span a small range of x and this range varies strongly with Q^2; see Fig. 12 of [1]. On the other hand, for all Q^2 bins the data are inside a narrow W interval

$$167 \text{ GeV}–232 \text{ GeV} \tag{18}$$

with a mean value of about $W_0 = 200$ GeV. Therefore, in the following we find it more convenient to consider F_L and F_2 as functions of W and Q^2 instead of x and Q^2.

Since we do not expect any large variation of the ratio $F_L(W, Q^2)/F_2(W, Q^2)$ for fixed Q^2 within the W interval (18) of the measurement we have averaged the H1 data [1] for given Q^2. In a first step for all H1 data points the ratio $F_L(W, Q^2)/F_2(W, Q^2)$ and its corresponding experimental uncertainty are calculated taking into account the correlation between the F_L and F_2 measurement as given in Table 22 in [1]. In a second step error weighted averages $\langle F_L(\langle W \rangle, Q^2)/F_2(\langle W \rangle, Q^2) \rangle$ are determined by combining ratios at constant Q^2 but different W values assuming that the individual measurements of the ratios are uncorrelated. Note that identical results are obtained by first averaging the F_L and F_2 values at constant Q^2 and then doing the ratio calculation. The averages are confronted with the bound (16) in Fig. 2. The numerical values of the data points in Fig. 2 are given in Appendix B.

We note firstly, that electromagnetic gauge invariance requires

$$\frac{F_L(W, Q^2)}{F_2(W, Q^2)} \to 0 \tag{19}$$

for $Q^2 \to 0$ at fixed W. The data indicate, indeed, a decrease of F_L/F_2 for small Q^2. Fitting F_L/F_2 with a constant value, as done in [1], does not seem very plausible physically, in view of (19).

The second point to note is that the data in Fig. 2 are rather close to the upper bound (16) from the dipole model, especially so for

$$3.5 \text{ GeV}^2 \leqslant Q^2 \leqslant 20 \text{ GeV}^2. \tag{20}$$

The bound (16) on F_L/F_2 can be improved if one takes into account that there is a non-vanishing contribution from charm quarks to F_L and F_2, see [31]. Specifically, considering massless u, d and s quarks, a massive c quark and neglecting b quarks we can derive certain allowed domains for the vector $\vec{V}(x, Q^2)$ (8) from the dipole model. Again these domains depend only on the known photon densities $w_{T,L}^{(q)}$, see (29)–(32), and on the non-negativity of the cross sections $\hat{\sigma}^{(q)}$, see (5). That is, for any dipole model with the standard photon probability densities $w_{T,L}^{(q)}$ the vector $\vec{V}(x, Q^2)$ must be inside the appropriate allowed domain for the given Q^2 value. A detailed description of how these domains are obtained has been given in [31]. The allowed domains can be understood as correlated bounds for the ratios F_L/F_2 and $F_2^{(c)}/F_2$. More precisely, one obtains for any given x and Q^2 an upper bound on F_L/F_2 which depends on the value of $F_2^{(c)}/F_2$ at the same kinematic point.

In Fig. 3 we show these allowed domains and the corresponding data. The bounds are calculated for a charm quark mass of $m_c = 1.23$ GeV. For each data point the corresponding ratio $F_2^{(c)}/F_2$ is obtained using NLO QCD calculations provided by the OPENQCDRAD package [33], again with a charm pole mass of $m_c = 1.23$ GeV. For this calculation the JR09FFNNLO parametrisation [34] of the proton parton density functions was used, which was found to describe HERA charm data [35] very well within the experimental correlated uncertainties of typically 3–9%. Here and in the following we do not consider the data point at $Q^2 = 1.5$ GeV^2 from [1] as it has an exceedingly large error. For the numerical values of the data in Fig. 3 see Appendix B.

The significance of the data points in relation to the bound can be seen more clearly from the quantity

$$\frac{\langle F_L/F_2 \rangle}{(F_L/F_2)|_{\text{bound}}} \tag{21}$$

which we plot in Fig. 4. For this figure the bound $(F_L/F_2)|_{\text{bound}}$ for each data point is extracted from Fig. 3 taking into account the corresponding value of $F_2^{(c)}/F_2$ at that kinematical point.

3. Discussion

We see from Figs. 2–4 that the data for $\langle F_L/F_2 \rangle$ as derived from [1] come very close to the bounds which result from the standard dipole picture. We now discuss the meaning of this observation from the points of view of both, a dipole-model enthusiast, and a dipole-model sceptic, respectively.

3.1. Dipole-model enthusiast's view

The dipole-model enthusiast will say that within the errors of the data the bounds are respected. Furthermore, he can use the data to give qualitative arguments concerning the behaviour of the dipole-proton cross sections for small and large radii r. Let us assume power behaviour of $\hat{\sigma}^{(q)}(r, \xi)$ for $r \to 0$ and $r \to \infty$,

$$\begin{aligned} &\hat{\sigma}^{(q)}(r, \xi) \propto r^a \quad \text{for } r \to 0, \\ &\hat{\sigma}^{(q)}(r, \xi) \propto r^{2-b} \quad \text{for } r \to \infty. \end{aligned} \tag{22}$$

Taking into account (10) we find that the integrals for F_2 and F_L in (4) are convergent if

$$a > 0 \quad \text{and} \quad b > 0. \tag{23}$$

Of course, with the usual assumptions of colour transparency for small r, implying $a = 2$, and of saturation for the dipole-proton cross sections for large r, implying $b = 2$, the requirements (23) are satisfied. From the experimental findings of Figs. 2 to 4 we can now give qualitative arguments based on the data, that the

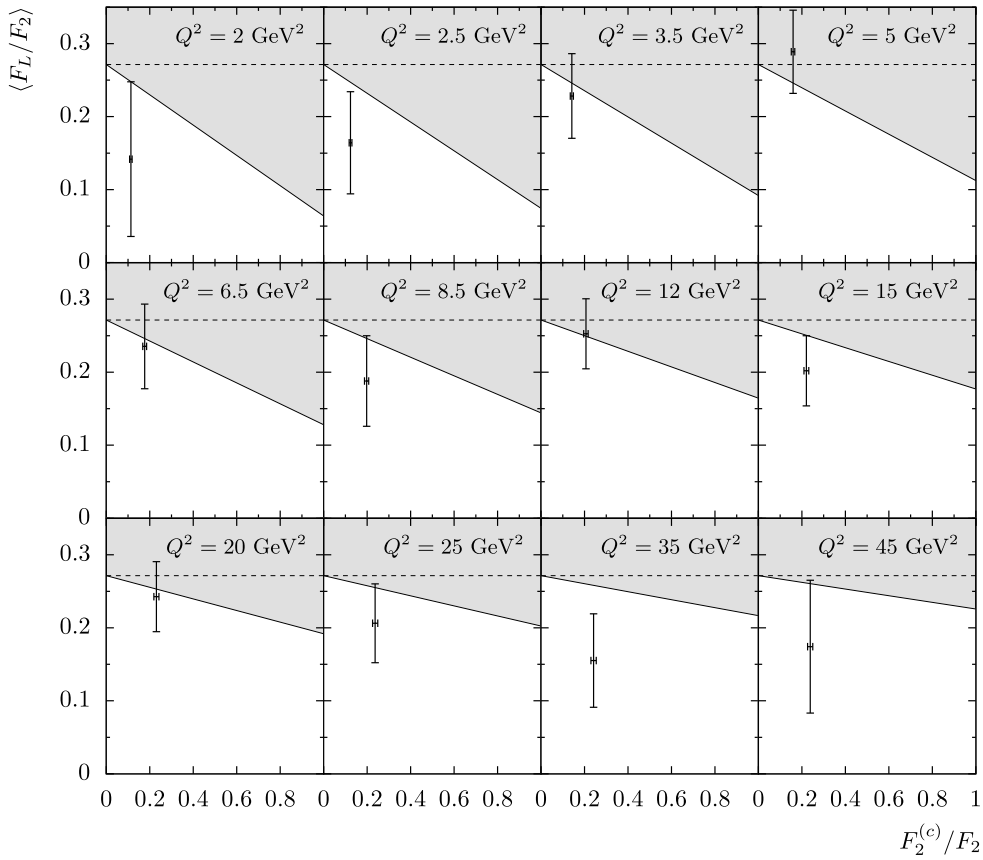

Fig. 3. The allowed domains and the data for $\langle F_L/F_2\rangle$ versus $F_2^{(c)}/F_2$ for $Q^2 = 2$ GeV^2 to $Q^2 = 45$ GeV^2. In the dipole model, the shaded areas are excluded by the correlated bounds for F_L/F_2 and $F_2^{(c)}/F_2$. The dotted line is the bound (16) on F_L/F_2 only.

exponents a and b in (22) cannot be too small. Indeed, for a small value of a the cross sections $\hat{\sigma}^{(q)}(r,\xi)$ would decrease only slowly for $r \to 0$ and this region of small r would contribute significantly in the integrals (4). But, as we see from the second plot in Fig. 1, the function $g(Q,r,0)$ is small there and this would lead to a small value for F_L/F_2, much below the bound (16), contrary to what is seen in the data. A similar argument applies to the exponent b in (23), considering the large r behaviour of $g(Q,r,0)$ in Fig. 1. Thus, the dipole-model enthusiast may hope that with more data it may even be possible to determine the exponents a and b from the data on F_L/F_2 directly without making model assumptions for $\hat{\sigma}^{(q)}(r,\xi)$.

3.2. Dipole-model sceptic's view

Let us now go over to the point of view of the dipole-model sceptic. He will note that some central values of the data for F_L/F_2 in Fig. 3 are, in fact, *above* the corresponding bound. If any of the measured points with $\langle F_L/F_2\rangle > (F_L/F_2)|_{\text{bound}}$ is confirmed, with corresponding small error, by further experiments then, as a clear consequence, the standard dipole picture would not be valid at this kinematic point. But what would be the consequences if the bound for F_L/F_2 is not *violated* but *saturated*?

For the sake of the argument we shall now for a moment *assume* that the bound for F_L/F_2 is reached in the Q^2 range (20). Clearly, this is not incompatible with the data, see Figs. 3 and 4. In this limiting case we get as consequence that the dipole-proton cross sections $\hat{\sigma}^{(q)}(r,\xi)$ in (4) can then only contribute at that particular r values where the functions $g(Q,r,0)$ and $g(Q,r,m_c)$ of (9) have their maximum. This is for both functions the case for

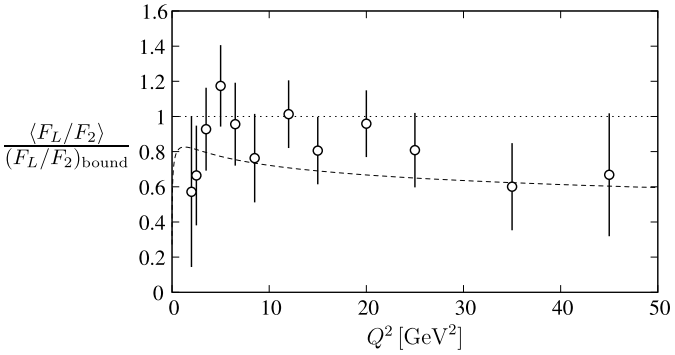

Fig. 4. The ratio $\langle F_L/F_2\rangle/(F_L/F_2)|_{\text{bound}}$, see (21), where the bound on F_L/F_2 results from taking into account the value of $F_2^{(c)}/F_2$ at the kinematical point of each data point. The dashed line is the ratio $(F_L/F_2)/(F_L/F_2)|_{\text{bound}}$ obtained in the Golec-Biernat–Wüsthoff model, see Section 3.

$$r \approx \frac{0.51\ \text{fm}}{\sqrt{Q^2/\text{GeV}^2}}. \tag{24}$$

We see this for $g(Q,r,0)$ from the second plot in Fig. 1 and this also holds for $g(Q,r,m_c)$. Thus, the ratio F_L/F_2 can be *equal* to the bound in the whole Q^2 interval (20) only if the cross section $\hat{\sigma}^{(q)}(r,\xi)$ is strongly peaked at the r value (24) for this whole Q^2 interval. That is, $\hat{\sigma}^{(q)}(r,\xi)$ must then have a δ function behaviour

$$\hat{\sigma}^{(q)}(r,\xi) \approx \delta\left(r - \frac{0.51}{Q}\right) \quad (r \text{ in fm},\ Q \text{ in GeV}). \tag{25}$$

The corresponding r values range from 0.27 fm for $Q^2 = 3.5$ GeV^2 to 0.11 fm for $Q^2 = 20$ GeV^2. With increasing Q the position of the delta function peak in (25) moves to smaller r values. As we have argued at length in [28,29,32], the correct energy variable in the dipole-proton cross section $\hat{\sigma}^{(q)}(r,\xi)$ is $\xi = W$. Since the data on F_L/F_2 is essentially at one value of $W \approx W_0 = 200$ GeV (more precisely, in the narrow range (18) around W_0) we get from (25) a Q^2 dependence in $\hat{\sigma}^{(q)}(r, W_0)$ which should *not* be there. The conclusion is that a saturation of the bound on F_L/F_2 in a whole Q^2 interval as in (20) is incompatible with the dipole model and the dipole-proton cross sections having the correct functional dependence $\hat{\sigma}^{(q)}(r, W)$.

With the – incorrect – choice of energy variable $\xi = x$ in $\hat{\sigma}^{(q)}(r,\xi)$ we get the following. Since the data on F_L/F_2 is essentially at $W = W_0$ (namely in the narrow range (18) around W_0), we have from (2)

$$x \simeq \frac{Q^2}{W_0^2}, \qquad Q \simeq \sqrt{x} W_0. \tag{26}$$

Inserting this in (25) gives

$$\hat{\sigma}^{(q)}(r,x) \approx \delta\left(r - \frac{0.51}{\sqrt{x} W_0}\right) \quad (r \text{ in fm},\ W_0 \text{ in GeV}). \tag{27}$$

Thus, there is in this case no immediate conflict with the functional dependence $\hat{\sigma}^{(q)}(r,x)$. But we note that as x *decreases* the peak of the cross section $\hat{\sigma}^{(q)}(r,x)$ in (25) shifts to *larger* values of r. This is in contrast to what one finds in popular dipole models, like the one invented by Golec-Biernat and Wüsthoff [7]. There, one assumes a dipole-proton cross section saturating at large r with an x-dependent saturation scale. But in that model for *decreasing* values of x the cross section $\hat{\sigma}^{(q)}(r,x)$ moves to *smaller* values of r, see Fig. 2 of [7]. This is in contradiction to what we found above in (27).

We were asked by a referee to discuss also the question how close specific dipole models may come to our bounds. To illustrate this issue we confront, as an example, the Golec-Biernat–Wüsthoff model with our correlated bounds in Fig. 4 where the ratio $(F_L/F_2)/(F_L/F_2)|_{\text{bound}}$ for this model is shown as the dashed line. Specifically, we consider the model of [7] with four flavours (see Table 1 there), that is

$$\begin{aligned}
&\hat{\sigma}^{(q)}_{\text{GBW}}(r,x) = \sigma_0\big[1 - \exp\big(-Q_s^2(x) r^2/4\big)\big],\\
&Q_s^2 = \left(\frac{x_0}{\tilde{x}}\right)^{\lambda} \text{GeV}^2, \qquad \tilde{x} = x\big(1 + 4m_q^2/Q^2\big),\\
&\sigma_0 = 29.12 \text{ mb}, \qquad \lambda = 0.277, \qquad x_0 = 0.41 \cdot 10^{-4}.
\end{aligned} \tag{28}$$

We take the quark masses slightly different from those chosen in [7], namely as $m_{u,d,s} = 0$ and $m_c = 1.23$ GeV, and consider constant $W = 200$ GeV. Also here, the bound on F_L/F_2 is computed from the value of $F_2^{(c)}/F_2$ obtained in the GBW model for the kinematical point defined by the corresponding Q^2. We see from Fig. 4 that the GBW model remains considerably below the bound, and its closest approach to the bound reaches only 80 % of it. Even that value is reached only in a very narrow Q^2 range. Evidently, the GBW dipole cross section is not of the delta-function form (27). As a consequence, the ratio F_L/F_2 computed in this model cannot be close to the bound for a sizeable Q^2 range, as is indeed confirmed numerically for this model. We have checked that very similar results are obtained for the GBW model with the parameters chosen in [1] and for the model of [14]. We emphasise that in this paragraph we only wanted to show how close one comes to the bounds in some specific, widely used dipole models. It is explicitly not our aim to provide a fit to the data with these models. An investigation of simultaneous fits to F_2, $F_2^{(c)}$ and F_L is certainly beyond the scope of the present Letter. The main purpose of our present Letter is a comparison of the data to the standard-dipole-model bounds.

The dipole-model sceptic could, furthermore, argue as follows. Since the bounds explored in the present Letter are just more or less satisfied by the data it will certainly pay to explore further rigorous bounds which can be constructed using the methods of [31]. One could, for instance, consider correlated bounds on F_L/F_2 at different Q^2 values. It remains to be explored if the standard dipole model survives such extended tests.

Finally, we would like to point out another issue that goes beyond the scope of the present study. This is the question of corrections to the standard dipole model. In [28,29] the dipole picture was investigated using functional methods. In particular, in (113) and (117) of [29] a general formula for the DIS amplitudes in the limit $W \to \infty$ at fixed Q^2 was given. These amplitudes were represented as integrals over photon wave functions plus rescattering terms times dipole-proton scattering amplitudes. The need of the rescattering terms is explained in Section 2 of [28] and is analogous to what one finds in the treatment of overlapping divergences in QED. From these results the assumptions leading to the standard dipole model were explicitly listed in Section 6 of [29]. The problem of going beyond this standard dipole picture by including, for instance, gluon emission from quark lines is the following. In the above framework diagrams with gluon emission from quark lines will contribute to all factors mentioned above, to the photon wave function, the rescattering term and the dipole-proton amplitude. But the latter is a nonperturbative object. Thus, for consistency, one would have to model the corrections one wants to consider also for this nonperturbative object. Most probably one will have then to give up for example the assumption that the quark and antiquark do not change their momenta when traversing the proton. Also the inclusion of diagrams of type (b) in Fig. 4 of [29], which will be necessary at some stage, leads one to the same conclusion. While an important step towards understanding part of the corrections to the dipole model was made by computing the photon wave function at NLO (see for example [36–39] and references therein) the other factors in the full amplitude are not known to any similar accuracy. Thus, unless one wants to restrict the whole description of photon wave functions, rescattering terms and dipole-proton scattering amplitudes to perturbation theory any quantitative statements on the magnitude of corrections to the bounds considered in the present Letter appear very difficult to us. In that situation it should be very useful to have rigorous tests of the standard dipole picture such that from the data we may learn if and where modifications are necessary and particularly important.

4. Summary

In this Letter we have derived fixed-Q^2 averages from the recent data on F_L/F_2. We have discussed the behaviour of these averages for $Q^2 \to 0$ in view of gauge invariance. The averages were compared with rigorous bounds derived in the framework of the standard dipole model. Within the experimental errors the bounds are satisfied. But the data is surprisingly close to the bounds for 3.5 GeV$^2 \leqslant Q^2 \leqslant 20$ GeV^2. We find it very remarkable that the high energy HERA data on F_L/F_2 at $W \approx 200$ GeV show a very different behaviour as compared to the fixed-target data on $R = \sigma_L/\sigma_T$. The latter were taken at a value of W that is an order of magnitude smaller. They were analysed in [29,30] where it was shown that they come close to or exceed the rigorous bounds of the standard dipole model only for $Q^2 \leqslant 2$ GeV^2. We have discussed the meaning of our findings for the HERA data

from the points of view of both, the dipole-model enthusiast and the sceptic. Clearly, if the central values of the data exceeding the bounds are confirmed with correspondingly small errors by further experiments, the standard dipole picture is ruled out at these kinematic points. We have, furthermore, shown that from data coming close to or maybe saturating the bounds in the Q^2 interval (20) one can draw very interesting conclusions on the behaviour of the dipole-proton cross sections. We have given arguments that these cross sections cannot be too large for the limits $r \to 0$ and $r \to \infty$ of the dipole size r. The enthusiast may interpret this as model-independent signatures pointing to colour transparency and saturation. We have explored the consequences of a possible exact saturation of the bounds in the whole Q^2 interval (20). We have shown that this leads then rigorously to a δ-function behaviour of the dipole-proton cross sections, that is, to cross sections vanishing everywhere except at one r value which is proportional to $1/Q$. Of course, such a behaviour would be hard to accept from the physics point of view and would present strain for the standard dipole picture. If such a behaviour is confirmed by further experiments with small errors one would have to examine which of the assumptions needed to arrive at the standard dipole model (listed in Section 6.2 of [29]) one needs to relax. But at present, given the errors of the data, δ functions for the cross sections $\hat{\sigma}^{(q)}(r,\xi)$ as in (25) and (27) are not really necessary and the widths of the distributions compatible with the data have to be explored. But this is beyond the scope of this Letter. We have restricted ourselves to demonstrating that the popular 4-flavour GBW model [7] for the dipole-proton cross section does not approach the correlated bound to more than about 80 % and is far from saturating the bound for any extended Q^2 range.

To summarise, we have demonstrated in our Letter that measurements of F_L/F_2 give very valuable information on the dipole picture, its validity, and potentially on questions like colour transparency and saturation of the dipole-proton cross section. The standard dipole picture is widely used, also outside DIS. Therefore, it should pay to investigate in detail its range of validity in as rigorous a way as possible, that is, to test the assumptions, spelled out in [29], underlying this picture. Thus, programs for future electron– and positron–proton scattering experiments (see for instance [40, 41]) certainly should foresee F_L measurements as an important item on the list of physics topics.

Acknowledgements

We are grateful to Sascha Glazov for providing data tables and information on correlated data uncertainties. We would like to thank Markus Diehl for useful discussions. The work of C.E. was supported by the Alliance Program of the Helmholtz Association (HA216/EMMI). The work of A.v.M. was supported by the Schweizer Nationalfonds (Grant 200020_124773/1).

Appendix A. Photon densities

The probability densities $w_{T,L}^{(q)}$ for the virtual photon in (4) are given by

$$w_T^{(q)}(r,Q^2) = \int_0^1 \mathrm{d}\alpha \sum_{\lambda,\lambda'} \left|\psi_{\lambda\lambda'}^{(q)T}(\alpha,\boldsymbol{r},Q)\right|^2, \tag{29}$$

$$w_L^{(q)}(r,Q^2) = \int_0^1 \mathrm{d}\alpha \sum_{\lambda,\lambda'} \left|\psi_{\lambda\lambda'}^{(q)L}(\alpha,\boldsymbol{r},Q)\right|^2, \tag{30}$$

where the squared photon wave functions (summed over quark helicities λ, λ') are

Table 1
Structure function ratios for different values of Q^2: $F_2^{(c)}/F_2$ from NLO QCD calculations [33] and averaged ratios $\langle F_L/F_2\rangle$ as derived from H1 measurements [1], see Section 2 for details.

Q^2 [GeV^2]	$F_2^{(c)}/F_2$	$\langle F_L/F_2\rangle$
1.5	0.102	0.12 ± 0.30
2	0.113	0.14 ± 0.11
2.5	0.124	0.16 ± 0.07
3.5	0.142	0.23 ± 0.06
5	0.159	0.29 ± 0.06
6.5	0.177	0.24 ± 0.06
8.5	0.198	0.19 ± 0.06
12	0.207	0.25 ± 0.05
15	0.220	0.20 ± 0.05
20	0.231	0.24 ± 0.05
25	0.237	0.21 ± 0.05
35	0.242	0.16 ± 0.06
45	0.238	0.17 ± 0.09

$$\begin{aligned}\sum_{\lambda,\lambda'} &\left|\psi_{\lambda\lambda'}^{(q)T}(\alpha,\boldsymbol{r},Q)\right|^2 \\ &= \frac{3}{2\pi^2}\alpha_{\mathrm{em}} Q_q^2 \left\{\left[\alpha^2+(1-\alpha)^2\right]\epsilon_q^2\left[K_1(\epsilon_q r)\right]^2 \right. \\ &\quad \left. + m_q^2\left[K_0(\epsilon_q r)\right]^2\right\}\end{aligned} \tag{31}$$

and

$$\sum_{\lambda,\lambda'} \left|\psi_{\lambda\lambda'}^{(q)L}(\alpha,\boldsymbol{r},Q)\right|^2 = \frac{6}{\pi^2}\alpha_{\mathrm{em}} Q_q^2 Q^2\left[\alpha(1-\alpha)\right]^2\left[K_0(\epsilon_q r)\right]^2 \tag{32}$$

for transversely and longitudinally polarised photons, respectively. Here $r = \sqrt{\boldsymbol{r}^2}$ with $\boldsymbol{r}$ denoting the two-dimensional transverse vector from the antiquark to the quark. Q_q are the quark charges in units of the proton charge, and K_0 and K_1 are modified Bessel functions. The quantity $\epsilon_q = \sqrt{\alpha(1-\alpha)Q^2 + m_q^2}$ involves the quark mass m_q. For a derivation of the photon wave functions see for example [29].

Appendix B. Data for $\langle F_L/F_2\rangle$ and $F_2^{(c)}/F_2$

Table 1 contains the numerical values of the data for $\langle F_L/F_2\rangle$ and $F_2^{(c)}/F_2$ used in Figs. 2 and 3. They have been obtained as described in Section 2. The error on $F_2^{(c)}/F_2$ is estimated to be 5%.

References

[1] F.D. Aaron, et al., Eur. Phys. J. C 71 (2011) 1579, arXiv:1012.4355 [hep-ex].
[2] O. Nachtmann, Elementary Particle Physics: Concepts and Phenomena, Springer-Verlag, Berlin, Heidelberg, 1990.
[3] L.N. Hand, Phys. Rev. 129 (1963) 1834.
[4] N.N. Nikolaev, B.G. Zakharov, Z. Phys. C 49 (1991) 607.
[5] N.N. Nikolaev, B.G. Zakharov, Z. Phys. C 53 (1992) 331.
[6] A.H. Mueller, Nucl. Phys. B 415 (1994) 373.
[7] K. Golec-Biernat, M. Wüsthoff, Phys. Rev. D 59 (1999) 014017, arXiv:hep-ph/9807513.
[8] K. Golec-Biernat, M. Wüsthoff, Phys. Rev. D 60 (1999) 114023, arXiv:hep-ph/9903358.
[9] J. Bartels, K. Golec-Biernat, H. Kowalski, Phys. Rev. D 66 (2002) 014001, arXiv:hep-ph/0203258.
[10] M. McDermott, L. Frankfurt, V. Guzey, M. Strikman, Eur. Phys. J. C 16 (2000) 641, arXiv:hep-ph/9912547.
[11] H.G. Dosch, T. Gousset, H.J. Pirner, Phys. Rev. D 57 (1998) 1666, arXiv:hep-ph/9707264.
[12] A. Donnachie, H.G. Dosch, Phys. Rev. D 65 (2002) 014019, arXiv:hep-ph/0106169.
[13] A.I. Shoshi, F.D. Steffen, H.J. Pirner, Nucl. Phys. A 709 (2002) 131, arXiv:hep-ph/0202012.

[14] E. Iancu, K. Itakura, S. Munier, Phys. Lett. B 590 (2004) 199, arXiv:hep-ph/0310338.
[15] J.R. Forshaw, G. Kerley, G. Shaw, Phys. Rev. D 60 (1999) 074012, arXiv:hep-ph/9903341.
[16] J.R. Forshaw, G. Shaw, JHEP 0412 (2004) 052, arXiv:hep-ph/0411337.
[17] J.R. Forshaw, R. Sandapen, G. Shaw, JHEP 0611 (2006) 025, arXiv:hep-ph/0608161.
[18] H. Kowalski, D. Teaney, Phys. Rev. D 68 (2003) 114005, arXiv:hep-ph/0304189.
[19] G. Watt, H. Kowalski, Phys. Rev. D 78 (2008) 014016, arXiv:0712.2670 [hep-ph].
[20] L. Motyka, K. Golec-Biernat, G. Watt, in: Proceedings of HERA and the LHC: 4th Workshop on the Implications of HERA for LHC Physics, Geneva, May 2008, p. 471, arXiv:0809.4191 [hep-ph].
[21] G. Cvetic, D. Schildknecht, B. Surrow, M. Tentyukov, Eur. Phys. J. C 20 (2001) 77, arXiv:hep-ph/0102229.
[22] D. Schildknecht, B. Surrow, M. Tentyukov, Phys. Lett. B 499 (2001) 116, arXiv:hep-ph/0010030.
[23] M. Kuroda, D. Schildknecht, Phys. Lett. B 618 (2005) 84, arXiv:hep-ph/0503251.
[24] M. Kuroda, D. Schildknecht, Phys. Lett. B 670 (2008) 129, arXiv:0806.0202 [hep-ph].
[25] D. Schildknecht, arXiv:1104.0850 [hep-ph].
[26] M. Kuroda, D. Schildknecht, Phys. Rev. D 85 (2012) 094001, arXiv:1108.2584 [hep-ph].
[27] J.L. Albacete, N. Armesto, J.G. Milhano, C.A. Salgado, Phys. Rev. D 80 (2009) 034031, arXiv:0902.1112 [hep-ph].
[28] C. Ewerz, O. Nachtmann, Annals Phys. 322 (2007) 1635, arXiv:hep-ph/0404254.
[29] C. Ewerz, O. Nachtmann, Annals Phys. 322 (2007) 1670, arXiv:hep-ph/0604087.
[30] C. Ewerz, O. Nachtmann, Phys. Lett. B 648 (2007) 279, arXiv:hep-ph/0611076.
[31] C. Ewerz, A. von Manteuffel, O. Nachtmann, Phys. Rev. D 77 (2008) 074022, arXiv:0708.3455 [hep-ph].
[32] C. Ewerz, A. von Manteuffel, O. Nachtmann, JHEP 1103 (2011) 062, arXiv:1101.0288 [hep-ph].
[33] A. Alekhin, J. Blümlein, S. Moch, OPENQCDRAD package, version 1.4, http://www-zeuthen.desy.de/~alekhin/OPENQCDRAD/.
[34] P. Jimenez-Delgado, E. Reya, Phys. Rev. D 79 (2009) 074023, arXiv:0810.4274 [hep-ph].
[35] H. Abramowicz, et al., H1 and ZEUS Collaborations, arXiv:1211.1182 [hep-ex].
[36] V.S. Fadin, D.Y. Ivanov, M.I. Kotsky, Nucl. Phys. B 658 (2003) 156, arXiv:hep-ph/0210406.
[37] J. Bartels, D. Colferai, S. Gieseke, A. Kyrieleis, Phys. Rev. D 66 (2002) 094017, arXiv:hep-ph/0208130.
[38] I. Balitsky, G.A. Chirilli, Phys. Rev. D 83 (2011) 031502, arXiv:1009.4729 [hep-ph].
[39] G. Beuf, Phys. Rev. D 85 (2012) 034039, arXiv:1112.4501 [hep-ph].
[40] C. Aidala, et al., The EIC Working Group, A high luminosity, high energy electron-ion-collider – A white paper prepared for the NSAC LRP 2007, http://web.mit.edu/eicc/DOCUMENTS/EIC_LRP-20070424.pdf.
[41] M. Klein, The LHeC Study Group, in: Proceedings of 35th International Conference on High Energy Physics ICHEP 2010, Paris, July 2010, PoS ICHEP 2010 (2010) 520.